Clim Dyn (2017) 48:1413–1429
DOI 10.1007/s00382-016-3149-9

Does vertical temperature gradient of the atmosphere matter for El Niño development?

Zeng-Zhen Hu[1] · Bohua Huang[2,3] · Yu-heng Tseng[4] · Wanqiu Wang[1] · Arun Kumar[1] · Jieshun Zhu[1,5] · Bhaskar Jha[1,5]

Received: 21 December 2015 / Accepted: 23 April 2016 / Published online: 3 May 2016

Abstract In this work, we examine the connection of vertical temperature gradient of the tropospheric atmosphere along the equator with El Niño–Southern Oscillation (ENSO) and the possible impact of the long-term change of the gradient. It is suggested that when the temperature anomalies in the lower troposphere are relatively warmer (cooler) than in the upper troposphere, the atmosphere is less (more) stable and favors an El Niño (a La Niña) event to develop. ENSO evolutions in 1997–1998 and 2014–2015 events are good examples of this relationship. They started from similar ocean anomaly states in the springs of 1997 and 2014, but developed into an extreme El Niño in 1997–1998 and a borderline El Niño in 2014–2015. That may be partially due to differences in the evolutions of the vertical temperature anomaly gradient in troposphere. Thus, in addition to the significant atmospheric response to ENSO, the preconditioning of vertical gradient of the tropospheric temperature due to internal atmospheric processes to some extent may play an active role in affecting ENSO evolution. The long-term trend with more pronounced warming in the upper troposphere than in the lower troposphere causes a reduction in the vertical temperature gradient in the troposphere. Moreover, unlike almost homogenous warm anomalies in the upper troposphere, the lower troposphere shows remarkable regional features along the equator during 1979–2014, with cold anomaly trends over the central and eastern Pacific Ocean associated with the so-called hiatus and some warm anomalies on its two sides in the east and west. This vertical and zonal distribution of the air temperature trends in the troposphere over the Pacific Ocean is consistent with the convection suppression over the central Pacific since 2000, implying a weakening of atmosphere and ocean coupling.

Keywords El Niño–Southern Oscillation · Vertical gradient of atmospheric temperature · Tropical convection · Long-term trend

1 Introduction

The El Niño–Southern Oscillation (ENSO) is the dominant mode of climate variability across the tropical Pacific Ocean on seasonal-to-interannual time scales (Rasmusson and Carpenter 1982; Kumar et al. 2014a) and a major contributor to global sea surface temperature (SST) variations (Kumar et al. 2014b). ENSO is also the most important source of potential predictability for global climate variations (National Research Council 2010; Wang et al. 2010). In other words, the variability and predictability in other tropical ocean basins and in the extratropical Pacific Ocean (Hu et al. 2013a, 2014; Jiang et al. 2013; Guan et al. 2014) are largely affected by SST anomalies in the central and eastern tropical Pacific Ocean associated with ENSO. Thus,

✉ Zeng-Zhen Hu
Zeng-Zhen.Hu@NOAA.GOV

1 Climate Prediction Center, NCEP/NWS/NOAA, 5830 University Research Court, College Park, MD 20740, USA

2 Department of Atmospheric, Oceanic, and Earth Sciences, College of Science, George Mason University, 4400 University Drive, Fairfax, VA 22030, USA

3 Center for Ocean-Land-Atmosphere Studies, 270 Research Hall, Mail Stop 6C5, George Mason University, 4400 University Drive, Fairfax, VA 22030, USA

4 Climate and Global Dynamics Division, National Center for Atmospheric Research, PO Box 3000, Boulder, CO 80307-3000, USA

5 Innovim, Greenbelt, MD, USA

ENSO plays the key role in global climate predictions on seasonal-interannual time scales.

Recently, a decline in ENSO prediction skill after 2000 has been noted (Wang et al. 2010; Barnston et al. 2012). The decline in skill is consistent with the weakening of the ENSO variability (Wang et al. 2010; Barnston et al. 2012; Hu et al. 2013b, 2016; Kumar and Hu 2014; Kumar et al. 2015), and is coincident with an interdecadal shift of ENSO characteristics around 1999/2000. McPhaden (2012) reported that, while warm water volume (WWV), a measure of oceanic heat content along the equatorial Pacific, leads ENSO SST anomalies by 2–3 seasons during the 1980s–1990s, the overall variability in WWV decreased and its lead time as the ENSO precursor also reduced to only one season during the 2000s. Similarly, Horii et al. (2012) argued that in comparison with 1981–2000, the relationship between WWV and ENSO weakened after 2000, especially during 2005–2011, and the discharge phases of WWV leading to La Niña events were less frequent after 2001.

A weakened relationship between WWV and ENSO in the past decade may be linked to a shift towards more frequent central Pacific versus eastern Pacific El Niños and the weakening of air–sea coupling in the tropical Pacific (McPhaden 2012; Horii et al. 2012; Hu et al. 2012a, 2016). Furthermore, in addition to the decrease of ENSO amplitude, ENSO also shifted to a relatively higher frequency regime (from 2 to 4 years averaged in 1979–1999 to 1.5–3 years after 2000; Hu et al. 2016). The suppressed variability and increased frequency, therefore, seem to be associated with the decrease of the ENSO prediction skill during 2000–2014.

Beyond documenting the change in ENSO characteristics after 2000, we also need to better understand why the ENSO variability was decreased and why fewer strong El Niño events occurred during 2000–2014. Some previous studies explored the role of change in the mean state both in the atmospheric boundary layer and ocean. For example, based on an observational analysis, Xiang et al. (2013) noted a decadal change that is characterized by a La Niña-like background pattern after late 1990s, and was associated with a strong divergence in the central Pacific atmospheric boundary layer. They argued that this anomalous wind divergence in the central Pacific shifted the anomalous atmospheric convection westward, leading to a westward shift of the anomalous westerly response, thereby preventing the eastward propagation of the SST anomaly after the late 1990s.

Hu et al. (2013b) documented a coherent interdecadal shift in both the variability and mean state in the tropical Pacific Ocean. They pointed out that, compared with 1979–1999, the interannual variability in the tropical Pacific atmosphere and ocean significantly weakened in 2000–2011. The change in the variability was then linked to the mean state of the tropical Pacific Ocean. Specifically, compared with 1979–1999, the zonal tilting of the equatorial thermocline became steeper during 2000–2011. The difference in the mean state of thermocline between the two periods was consistent with warmer (colder) SSTs, increased (decreased) precipitations, enhanced (suppressed) convections in the western (central and eastern) tropical Pacific, and stronger (weaker) Walker circulations during 2000–2011 (1979–1999). They emphasized the role of mean state change, and proposed that the combination of a steeper thermocline slope with stronger surface trade winds may hamper the zonal migration of the warm water along the equatorial Pacific. As a consequence, the variabilities in WWV and ENSO decreased. They further argued that both too large and too small thermocline slopes (corresponding too strong and too weak wind stress) can potentially lead to suppression in ENSO variability, a hypothesis that was verified by model sensitivity experiments.

An issue with above investigations is that the analysis points to consistency, but not to causal relationships. In this analysis we start with the hypothesis that low-frequency changes in the atmosphere in the troposphere may play a role in altering ENSO behavior (such as fewer strong El Niño events in 2000–2014). For example, tropical convection (which plays an important and active role in air–sea coupling) relies not only on the thermal condition of the ocean surface, but also on atmospheric environment, such as low-level atmospheric convergence, zonal temperature gradient and vertical temperature gradient (stratification, or profile) in the troposphere. Previous studies have suggested that variations in the mid and upper troposphere can be an independent factor influencing the tropical climate variability. For instance, the downward propagating temperature anomalies near the tropopause originating from the stratosphere associated with the quasi-biennial oscillation (QBO) may modulate deep convection in the tropics through altering atmospheric stability (e.g., Collimore et al. 2003; Huang et al. 2012; Hu et al. 2012c). Similarly, a recent modeling study by Nie and Sobel (2015) suggested that the QBO-induced temperature anomalies in the upper troposphere could alter the profile of the large-scale vertical motion and the vertical energy transport throughout the troposphere.

In this work, two questions are addressed: (1) what is the connection of the atmospheric temperature in the troposphere along the equator with ENSO? And (2) what role does the long-term change of atmosphere temperature in the troposphere along the equator play in the ENSO feature change in 2000–2014? To the best of our knowledge, the linkage of vertical structure of atmospheric temperature with the ENSO evolution has not been explicitly investigated in detail.

The paper is organized as follows. The data used in the analysis are described in Sect. 2. In Sect. 3, through lead-lag (partial) correlations in observations and model simulations, the connection of convection over the central Pacific with SST and the atmosphere temperature in the troposphere is investigated. The long-term change of the atmospheric temperature gradient along the equatorial Pacific in the troposphere, and its possible impact on the convection, and the fact of fewer strong El Niño in 2000–2014 are also discussed. A summary and discussions appear in Sect. 4.

2 Data and methodology

The primary variable analyzed in this work is the atmospheric temperature from surface to 100 hPa on a 2.5° × 2.5° grid from reanalysis data of the NCEP and Department of Energy (NCEP/DOE; Kanamitsu et al. 2002). In addition, monthly mean outgoing long-wave radiation (OLR) data on a 2.5° × 2.5° grid from Liebmann and Smith (1996) are also analyzed. OLR is used as a proxy for convective activity over the tropical oceans. The data used in this work span the period of Jan. 1979–Dec. 2014. To target the anomalous relationships, except in Fig. 10 (that mean anomaly is referred to climatology in 1979–2014) and Fig. 11, in all other calculations, monthly mean anomalies with respect to monthly climatologies in 1981–2010 are used.

Variabilities of two indices are analyzed (Fig. 1a). One is the conventional Niño3.4 index (curve in Fig. 1a), which is the average of OIv2 SST anomalies in (5°S–5°N, 170°W–120°W) (rectangle in Fig. 1c) (Reynolds et al. 2002). The Niño3.4 index represents the anomalous SST variability in the central and eastern Pacific as well as the variations of global oceans associated with ENSO (Fig. 1c) (Barnston et al. 1997). The other index is the so-called central Pacific OLR (CP-OLR) index (shading in Fig. 1a), which is defined as the OLR anomalies averaged in 5°S–5°N, 170°E–140°W (the rectangle in Fig. 1b). According to L'Heureux et al. (2015), the CP-OLR index is representative of the deep-convective variability in the central and eastern tropical Pacific, as well as the global variations connected to ENSO.

To isolate the connection of the tropospheric temperature variation with the tropical convection without the influence from ENSO, lead-lag *partial* correlations between the tropical convection and vertical atmospheric temperature anomalous gradient after removing ENSO are computed (Pedhazur 1997). The partial correlation of A and B adjusted for C is:

$$r_{\mathrm{ABC}} = \frac{r_{\mathrm{AB}} - r_{\mathrm{AC}} r_{\mathrm{BC}}}{\sqrt{(1 - r_{AC}^2)(1 - r_{BC}^2)}} \tag{1}$$

where, r_{AB}, r_{AC}, and r_{BC} are the correlations between A and B, A and C, B and C, respectively. Here, A is the CP-OLR index, B is a vertical atmospheric temperature gradient index that will be defined in Sects. 3.2 and 3.3 is the Niño3.4 index.

Also, an atmospheric model simulation forced by *climatological* SST and sea ice averaged in 1981–2010 is analyzed. The model simulations are from the atmospheric component (Global Forecast System; GFS) of the NCEP Climate Forecast System version 1 (Saha et al. 2006). The model integration is 30 years.

3 Results

Figure 1b, c display the correlations between the CP-OLR index and global OLR anomalies and between the Niño3.4 index and global SST anomalies, respectively. In addition to the similarity of the spatial patterns of the correlations shown in Fig. 1b, c, there are clear differences. For example, in the central and eastern Pacific, the positive correlations have wider meridional extension for the correlations between SST anomaly and Niño3.4 index (Fig. 1c) than that for the correlations between OLR anomaly and CP-OLR index (Fig. 1b). Furthermore, the correlation patterns in the Indian and Atlantic Oceans, as well as in the North and South Pacific also have obvious differences. This suggests that although SST and OLR anomalies in the central and eastern tropical Pacific Ocean, represented by the CP-OLR and Niño3.4 indices (Fig. 1a), respectively, are connected, their teleconnections in remote regions differ. It may also imply that the convection activity is affected by other factors (such as, atmospheric stratification, humidity, convergence and divergence) in addition to SST.

From the time series of the CP-OLR index (shading in Fig. 1a), we note that the ENSO-related anomalous convection (i.e., negative CP-OLR values) in the central Pacific was generally weak in 2000–2014 compared to that before 2000. In contrast to large fluctuations between positive and negative values before 2000, positive OLR anomalies were dominant during 2000–2014. Furthermore, for the El Niño events during 2000–2014, the corresponding negative OLR anomaly had smaller amplitude and persisted for a shorter duration, even for the relatively strong El Niño event in 2009–2010, compared with El Niño events during 1979–1999 (Figs. 1a, 2; Table 1). For example, mean values of CP-OLR and Niño3.4 indices as well as El Niño duration (see the filled rectangles at the top of Fig. 1a) averaged for El Niño events occurring in 1979–1999 are −19.6 W/m^2, 1.17 °C, and 11.8 months, respectively. The corresponding numbers in 2000–2014 are −8.8 W/m^2, 0.812 °C, and 8.25 months, respectively. These differences between the

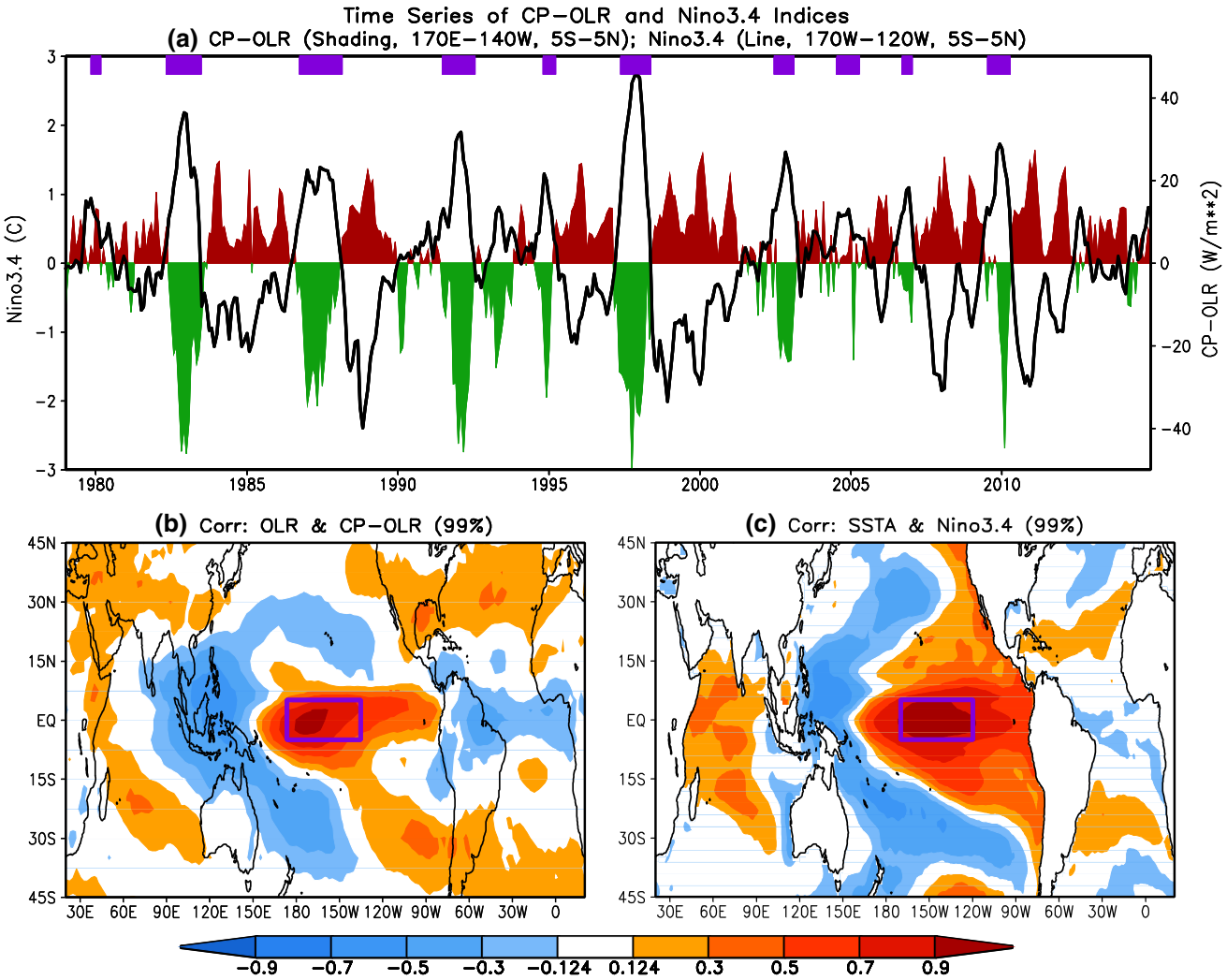

Fig. 1 Monthly mean of **a** CP-OLR (*shading*) and Niño3.4 (*curve*) indices in Jan. 1979–Dec. 2014, and correlations **b** between the CP-OLR index and OLR anomalies, **c** between the Niño3.4 index and SST anomalies. The CP-OLR index is defined as the OLR anomalies averaged in (5°S–5°N, 170°E–140°W; see the *rectangle* in **b**), and the Niño3.4 index is the average of SST anomalies in (5°S–5°N, 170°W–120°W; see the *rectangle* in **c**). The units are W/m^2 and °C for the CP-OLR and Niño3.4 indices in **a**, respectively. The *filled rectangles* at the top of **a** represent the duration of each El Niño event used in the calculations of Table 1. *Shading* in **b**, **c** represents the significant correlation at 99 % confidence level using the *T* test

two periods are quite remarkable (Table 1). We should mention that the El Niño events chosen here are based on the definition of Climate Prediction Center (CPC) (http://www.cpc.ncep.noaa.gov/products/analysis_monitoring/ensostuff/ensoyears.shtml). Contrarily, the differences of OLR anomalies between 1979–1999 and 2000–2014 for La Niña events (Fig. 2) are not as pronounced as for El Niño events.

The weakened OLR variability in El Niño years in 2000–2014 is consistent with overall reduction in variability of tropical atmosphere and ocean coupled system as documented by McPhaden (2012), Horii et al. (2012), Hu et al. (2013b), Xiang et al. (2013), and Kumar and Hu (2014). The lack of strong convections associated with El Niño events during 2000–2014 may be partially associated with a westward shift of the mean convective activity (Hu et al. 2013b), and also implies a weakened basin–wide air–sea interaction or the Bjerknes (1969) air–sea feedback normally seen in an El Niño development (Hu et al. 2016). Further, a shift to high frequency of the CP-OLR index (shading in Fig. 1a) is consistent with the fact that the tropical Pacific coupling system shifted to a higher-frequency regime in 2000–2014 noted by Hu et al. (2016). We hypothesize that, in additional to the forcing from the ocean thermal condition, the atmosphere environment (such as vertical and zonal temperature gradients), to some extent, may have played an active role in altering the characteristics of tropical convection development, and thus,

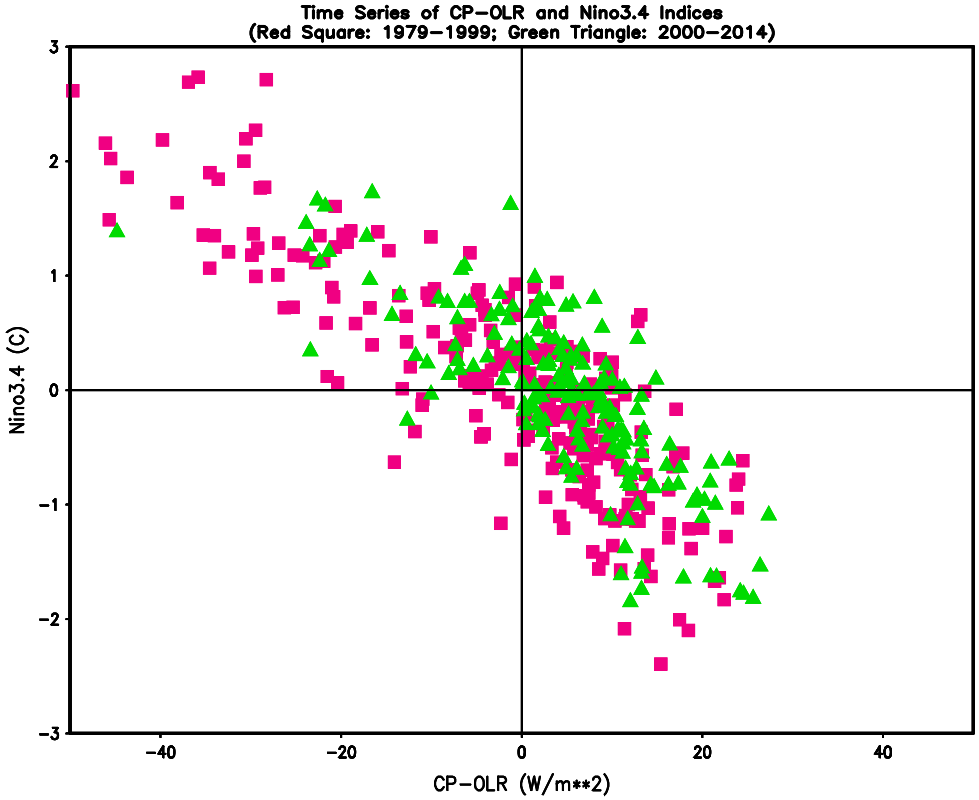

Fig. 2 Scatter of CP-OLR and Niño3.4 indices during Jan. 1979–Dec. 1999 (*red square*) and Jan. 2000–Dec. 2014 (*green triangle*)

Table 1 Mean values of CP-OLR and Niño3.4 indices as well as El Niño duration (see the filled rectangles at the top of Fig. 1a) averaged in El Niño years in 1979–1999 and 2000–2014 and their differences

El Niño year mean	1979–1999	2000–2014	Differences: (2000–2014) to (1979–1999)
CP-OLR (W/m^2)	−19.6	−8.8	10.8
Niño3.4 SSTA (°C)	1.17	0.812	−0.358
El Niño duration (months)	11.8	8.25	−3.55

affect the air–sea coupling in the tropical Pacific and the ENSO development.

3.1 Significant response of atmospheric temperature in the troposphere to ENSO

Figure 3 shows the lead and lag correlations between the CP-OLR index and tropospheric temperature anomaly along the equator averaged in 5°S–5°N. We should point out that when convection is active, which corresponds to below normal OLR, regions with positive (negative) correlations correspond to cold (warm) anomalies of temperature, and vice versa.

For tropospheric temperature leading the CP-OLR index, negative correlation presents over the central and eastern tropical Pacific and positive correlations are found over the western tropical Pacific, tropical Indian and Atlantic Oceans (Fig. 3a–c). Physically, preceding the above-normal convection (i.e., negative OLR anomalies) in the central Pacific, troposphere warms over the central and eastern tropical Pacific and cools over the western tropical Pacific, tropical Indian and Atlantic Oceans. The tropospheric warm anomalies are largely confined to the lower troposphere and cold anomalies occur in the whole column between the surface and 100 hPa. These results are generally consistent with lead and lag correlations between the Niño3.4 index and air temperature anomaly along the equator averaged in 5°S–5°N (not shown).

At zero month lag, when convection is above normal (negative OLR anomaly), the warm anomalies intensify and extend into the whole troposphere, and the cold anomalies over the tropical Indian and Atlantic Oceans weaken. The strengthened and vertically extended warm anomalies are due to heat release from enhancement in convection in the central Pacific that are dispersed to the entire tropics. Meanwhile, the cold anomalies over the central and western tropical Pacific strengthen in the lower troposphere and weaken in the mid and upper troposphere. The lag correlations show that after above-normal convections (Fig. 3e, f) and positive Niño3.4 SST anomaly (not shown), the warm anomalies over the central and eastern Pacific weaken, but spread to the tropical Indian and eastern Atlantic Oceans. This is consistent with the delayed atmospheric response to

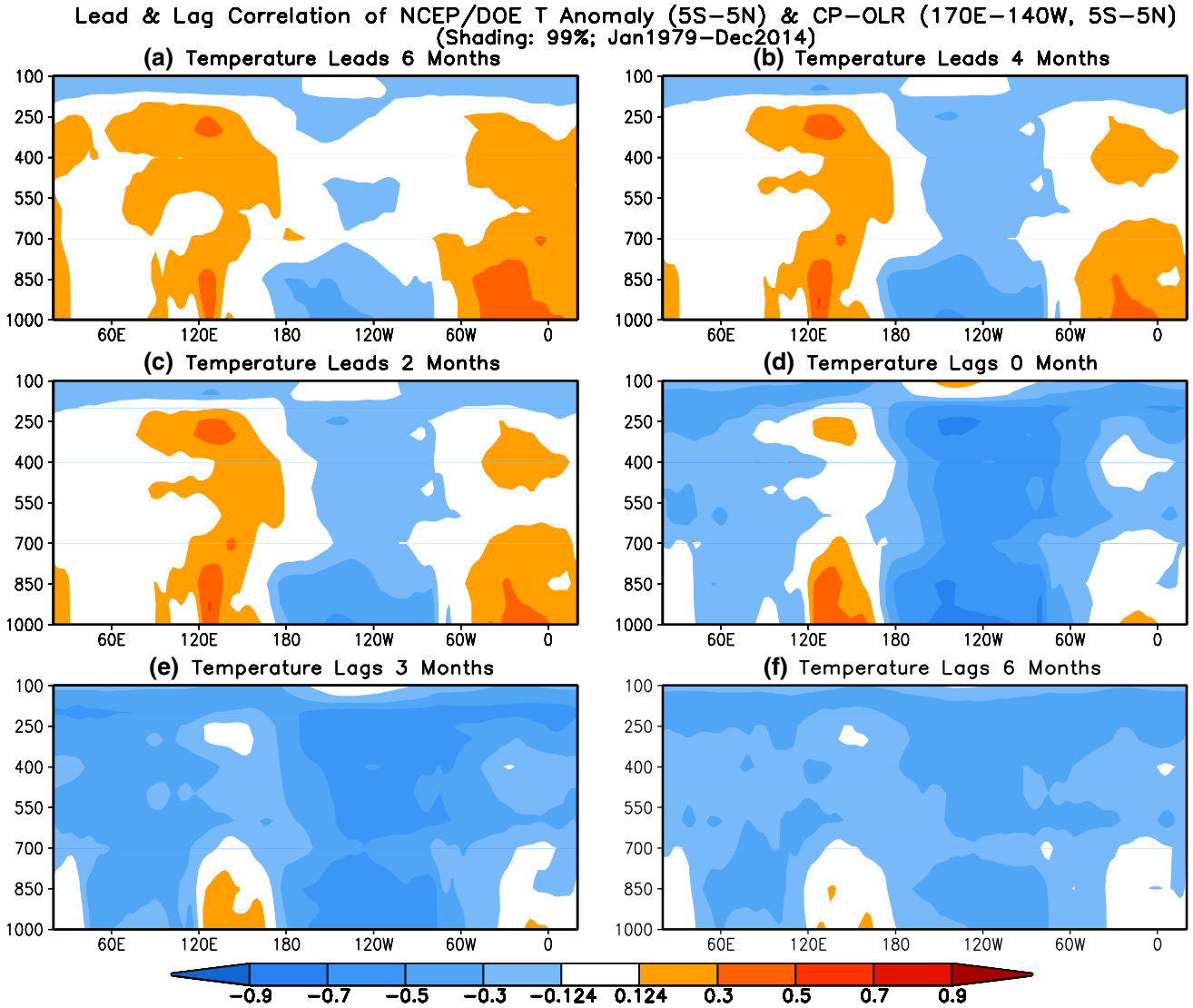

Fig. 3 Lead and lag correlations between the CP-OLR index and air temperature anomaly referred to climatology in 1981–2010 along the equator averaged in 5°S–5°N. **a**–**d** are the correlations for the temperature leading the CP-OLR index by 6, 4, 2, 0 months, and **e**, **f** are the correlations for the temperature lagging the CP-OLR index by 3 and 6 months, respectively. *Shading* represents the significant correlation at 99 % confidence level using the *T* test

ENSO documented by Kumar and Hoerling (2003). For the mechanism, as proposed by Chiang and Sobel (2002) and Sobel et al. (2002), the troposphere temperature anomaly alters moisture convection and then affects the communication of the tropospheric temperature signal caused by ENSO to the remote regions of ocean surface.

To further demonstrate the connection of ENSO with the tropospheric temperature, Fig. 4 shows the lead-lag correlations of temperature anomalies at 250 and 1000 hPa with the CP-OLR and Niño3.4 indices. The temperature anomaly is represented by average in (5°S–5°N, 170°E–60°W) (which is the region with the highest correlations in Fig. 3d) at 250 and 1000 hPa and is referred to as T250 and T1000, respectively. The results suggest that with the development of ENSO, lower tropospheric temperature along the equator evolves concurrently, and then the anomaly of the same sign is observed in the upper troposphere a few months later. That is consistent with the delayed atmospheric response to ENSO (Kumar and Hoerling 2003) that temperature signal associated with ENSO propagates from the low to the upper troposphere through the heat release associated with deep convection in response to SSTs.

3.2 Possible influence of atmosphere temperature vertical gradient on ENSO

From the analyses in the previous subsection, we see the evidence of the significant response of the tropospheric

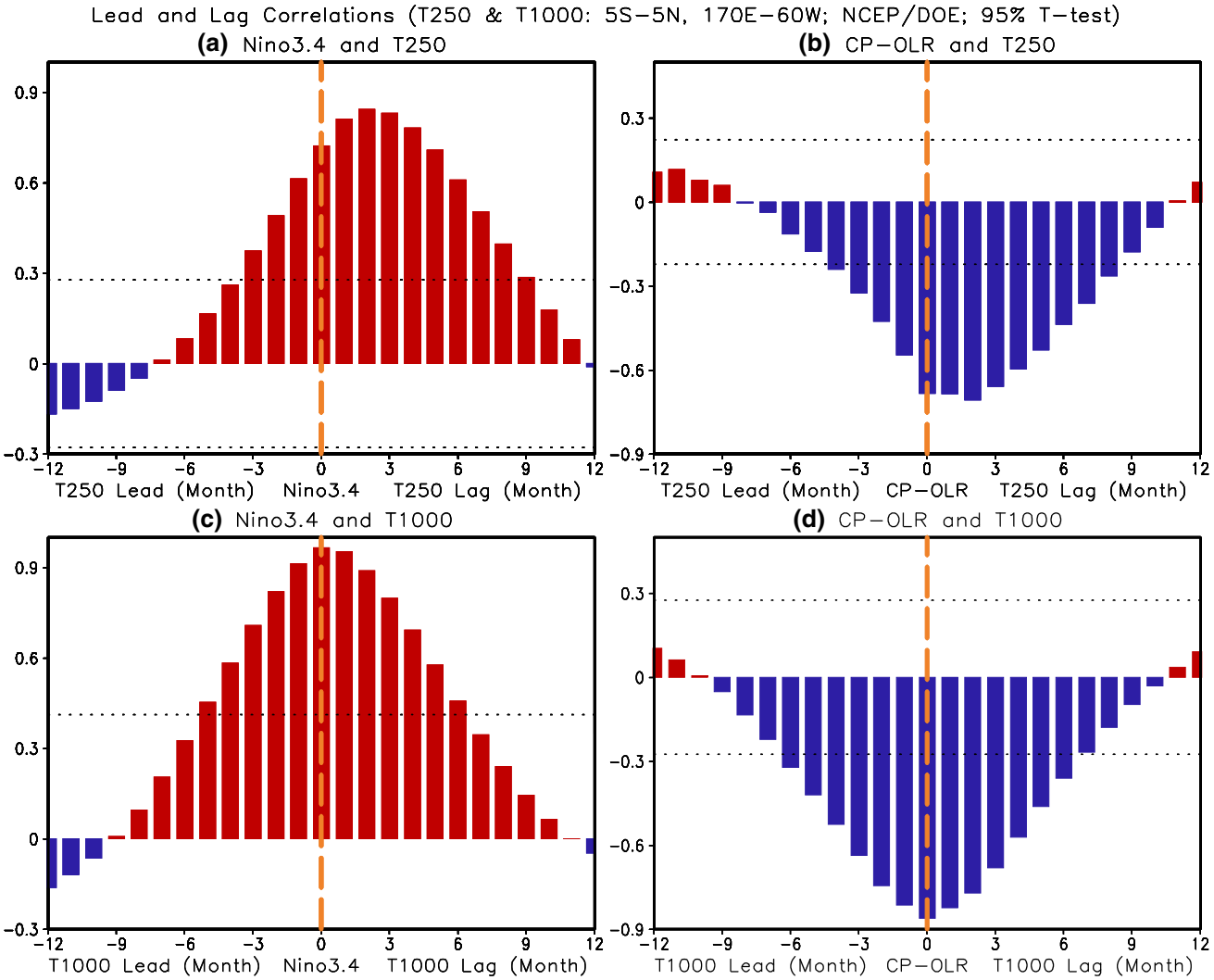

Fig. 4 Lead-lag correlations between **a** the Niño3.4 index and T250, **b** the CP-OLR index and T250, **c** the Niño3.4 index and T1000, and **d** the CP-OLR index and T1000. T250 and T1000 represent temperature anomaly at 250 and 1000 hPa averaged in (5°S–5°N, 170°E–60°W), respectively. Negative (positive) numbers in the *x* axis represent months of T250/T1000 leading (lagging) the Niño3.4 index in **a**, **c**, and leading (lagging) the CP-OLR index in **b**, **d**. *Dotted lines* represent the significance at 95 % confidence level using the *T* test. In the significance test, independent sample numbers are used following Bretherton et al. (1999)

temperature to ENSO. Now, we ask if there are any impacts of the tropospheric temperature, in particular the vertical temperature gradient, on an ENSO evolution. To investigate the possible impact, the lead and lag correlations among the CP-OLR index, the Niño3.4 index, and vertical temperature anomaly gradient index are calculated and shown in Fig. 5. Here, the vertical temperature anomaly gradient index is defined as the temperature anomaly difference between 250 and 1000 hPa averaged in (5°S–5°N, 170°E–60°W).

From Fig. 5b, we note that maximum negative correlation presents when the vertical temperature gradient index leads the Niño3.4 index by 3 months, and maximum positive correlation occurs when the vertical temperature gradient index lags the Niño3.4 index by 6–7 months. The existence of the negative correlation may be due to the fact that T1000 is a variable close to the surface and has very strong simultaneous correlation with Niño3.4 and meanwhile the correlation between T250 and Niño3.4 peaks at a lag of a few months. The correlation pattern shown in Fig. 5b may be a result of different delay time at different layer in the tropospheric temperature response to ENSO. On the other hand, both factors may play some roles for the vertical temperature gradient to affect or feedback to the ENSO evolution. That will be further examined later. In fact, the causes of the temperature vertical gradient affecting the atmospheric stability/stratification may also result from the extratropical forcings (e.g., Ding et al. 2015a, b), that are beyond the scope of this paper. The maximum

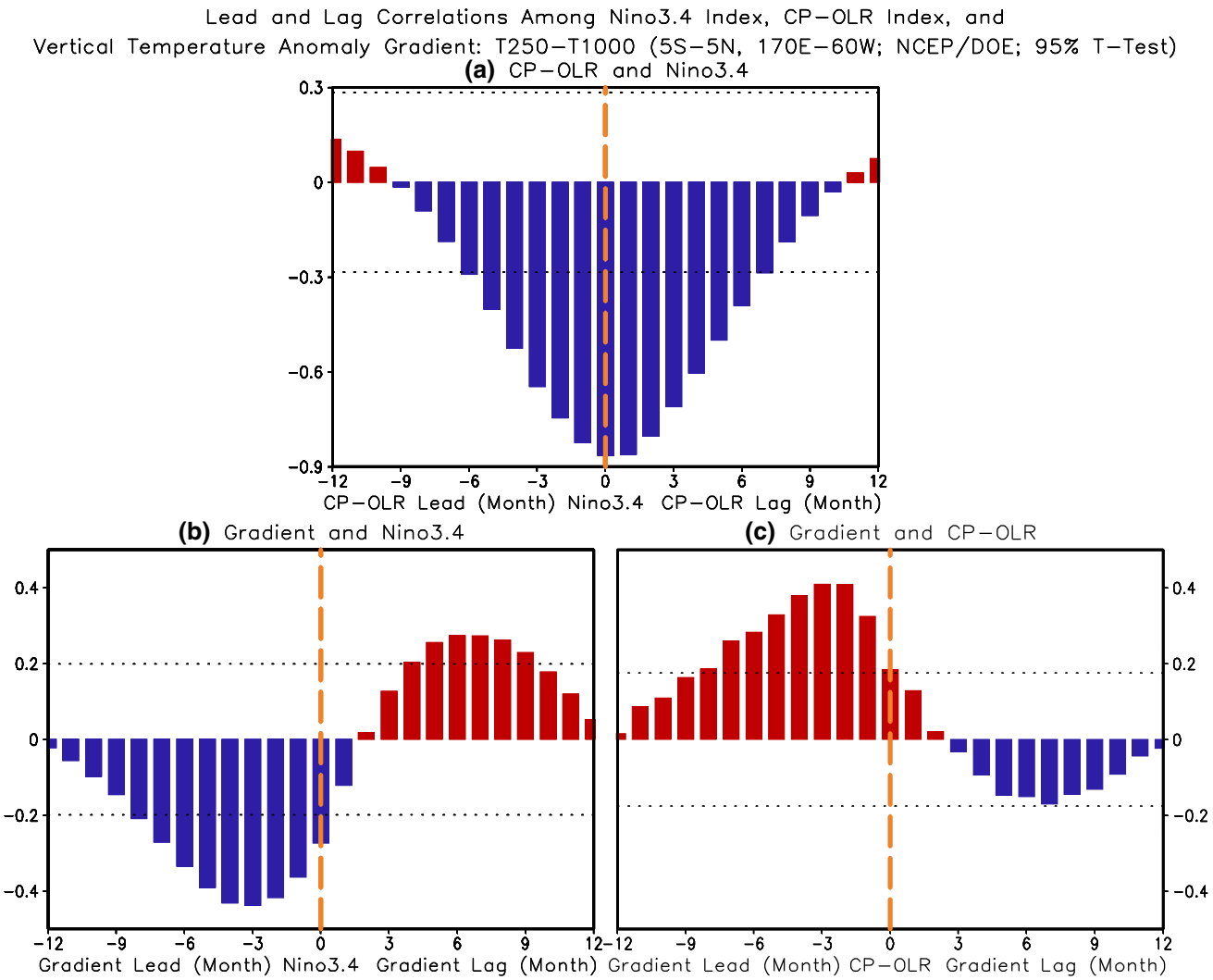

Fig. 5 Lead-lag correlations between **a** the CP-OLR and Niño3.4 indices, **b** the Niño3.4 index and vertical temperature anomaly gradient index, and **c** the CP-OLR index and the vertical temperature anomaly gradient index. The vertical temperature anomaly gradient index is defined as the temperature anomaly difference between 250 and 1000 hPa averaged in (5°S–5°N, 170°E–60°W). Negative (positive) numbers in the *x* axis represent months of the CP-OLR index leading (lagging) the Niño3.4 index in **a**, the vertical temperature anomaly gradient index leading (lagging) the Niño3.4 index in **b**, and the vertical temperature anomaly gradient index leading (lagging) the CP-OLR index in **c**. *Dotted lines* represent the significance at 95 % confidence level using the *T* test. In the significance test, independent sample numbers are used following Bretherton et al. (1999)

positive correlation is likely a consequence of heat release of condensation in the upper layer due to the deep convections associated with ENSO and a delay in upper tropospheric warm anomalies (Fig. 4). From the CP-OLR perspective, maximum positive correlation is seen when the vertical temperature gradient index leads the CP-OLR index by 2–3 months, and maximum negative correlation is observed with smaller amplitude when the vertical temperature gradient index lags the CP-OLR index by 7 months (Fig. 5c). This is consistent with the result in Fig. 5a that the correlation between the CP-OLR and Niño3.4 indices is negative and peaks at 0–1 month lag of the CP-OLR to Niño3.4 indices.

As we know, the atmospheric stability/stratification affects the atmospheric convection development. Nevertheless, the correlations shown in Figs. 3, 4 and 5 may be due to the combination of the heat release associated with convection forced by ocean surface heating and the impact of the stability on the convection due to other internal atmospheric processes. To exclude the influence of ENSO and to single out the connection between deep convection and troposphere stratification, Fig. 6 shows the lead-lag *partial* correlations (Pedhazur 1997; also see Eq. (1)) between the CP-OLR and the vertical temperature anomaly gradient indices adjusted for the Niño3.4 index. The partial correlations are significant and positive while the vertical

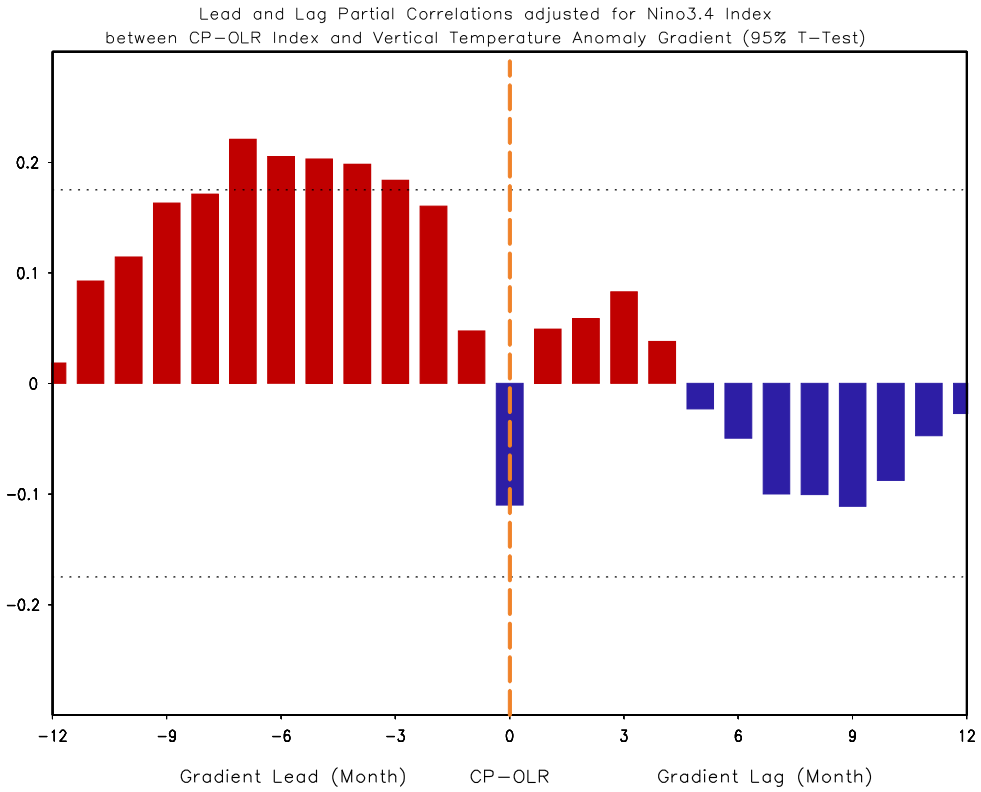

Fig. 6 Lead-lag partial correlations between CP-OLR index and the troposphere temperature differences between 250 and 1000 hPa averaged in (5°S–5°N, 170°E–60°W) adjusted for Niño3.4 index. *Dotted lines* represent the significance at 95 % confidence level using the *T* test. In the significance test, independent sample number is used following Bretherton et al. (1999)

temperature anomaly gradient index leads the CP-OLR index. This indicates that under the circumstance excluding the influence of ENSO associated processes, stability variations of the tropospheric atmosphere do affect the convective activity on seasonal time scales. The leading positive correlations here suggest that stable (unstable) troposphere suppresses (favors) the deep convection development. The partial correlation values (Fig. 6) are smaller than the corresponding correlations shown in Fig. 5c, suggesting that if the influence of ENSO is included, the connection between the deep convections and troposphere stratification is strengthened.

To further examine the connection between the vertical temperature stratification and convection anomalies, an atmospheric model (NCEP GFS) experiment forced by *climatological* SST and sea ice is analyzed. In the experiment, not only the influence of ENSO-associated SST anomaly but also other potential oceanic feedback on the vertical temperature profile is excluded because of the use of the climatological SST. Then, the lead-lag correlations between the CP-OLR and vertical temperature gradient indices (Fig. 7) show the connection in the model between two indices in the circumstance without the influence of ENSO. The correlations are positive when the vertical temperature gradient index leads the CP-OLR index by 5–11 months. The correlations become negative when the vertical temperature gradient index leads the CP-OLR index by 1 month to until lag by 2 months. When the vertical temperature gradient index leads the CP-OLR index, the positive correlations in the model experiment (Fig. 7) are generally consistent with that in the observations (Figs. 5c, 6). We should point out that in the model experiment, due to the specification of climatological SST, variability of temperature at 1000 hPa (T1000) in the tropical Pacific is significantly reduced (not shown). The variation of the vertical temperature gradient index defined in this work is dominated by the anomaly of T250. The model results support the argument that stable (unstable) troposphere suppresses (favors) the deep convection development, implying the impact of tropospheric stability on the convection evolution. However, in addition to noisier of the correlations in Fig. 7, the amplitudes of the correlations are smaller in Figs. 6 and 7 than in Fig. 5c, suggesting that, compared with the influence of the troposphere temperature variability on the convection, the impact of ENSO associated SST anomaly on the troposphere temperature variability is more significant and dominant. Furthermore, there are obvious differences between Figs. 6 and 7, such as the remarkable differences of the correlations when the gradient index leads the CP-OLR index by 1–5 months, that may be due to impact of sampling error, and/or an indication of default or bias of the model and/or reanalysis in capturing the connection between the tropospheric stratification and convection variations.

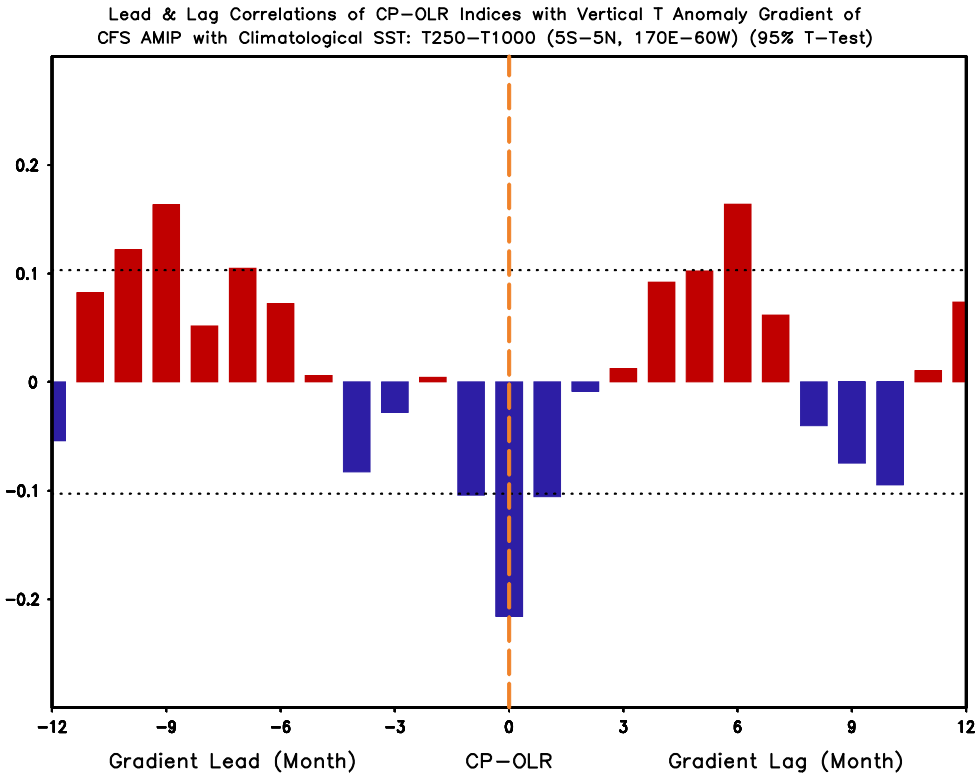

Fig. 7 Same as Fig. 5c, but for lead-lag correlations of the troposphere temperature differences between 250 and 1000 hPa averaged in (5°S–5°N, 170°E–60°W) in AMIP run forced by climatological SST with CP-OLR index. *Dotted lines* represent the significance at 95 % confidence level using the *T* test. In the significance test, independent sample number is used following Bretherton et al. (1999)

These lead and lag correlations in both the observations and model simulations suggest that when upper level (250 hPa) temperature anomaly is relatively cooler (warmer) than that in the lower level (1000 hPa), corresponding to negative (positive) vertical temperature anomaly gradient, the atmosphere is more (less) unstable and deep convections are more enhanced (suppressed). Putting this connection in the context of ENSO evolution, with favorable/unstable (unfavorable/stable) tropospheric stratification for convection development, an El Niño (a La Niña) is favored to develop through positive feedback among convections, lower and upper level winds and SST (so-called Bjerknes feedback, Bjerknes 1969). In other words, Bjerknes feedback requires mediation via convective activity, and if tropospheric stability is not conducive for convection, Bjerknes feedback may not sustain. Thus, the vertical temperature anomaly gradient in the troposphere, via enhancing or suppressing deep convections, may affect the ENSO evolution. In addition to the significant response of the tropospheric temperature to ENSO as analyzed in last subsection and previous studies (e.g., Chiang and Sobel 2002), the vertical temperature anomaly gradient in the troposphere seems sometime an active and important player at intraseasonal time scale in the coupling process during ENSO evolution.

The ENSO evolutions in 2014–2015 and 1997–1998 are two examples that are consistent with the above statistical relationship. In the early spring of 2014, subsurface ocean warm anomalies were even stronger than that in the same season of the 1997/1998 El Niño (http://origin.cpc.ncep.noaa.gov/products/GODAS/ocean_briefing_gif/global_ocean_monitoring_2014_05.pdf), the strongest El Niño event in the instrumental record. On the other hand, zonal atmospheric temperature gradient in the lower troposphere cross the tropical Pacific was weak. Meanwhile, positive anomaly of atmosphere temperature in the central tropical Pacific in the troposphere above 750 hPa was much larger than that below 750 hPa (Fig. 8c). According to the statistical relation, such zonal and vertical temperature gradient patterns in the tropical Pacific do not favor convection development. Eventually, the basin-wide air–sea interaction or the Bjerknes (1969) like air–sea feedback cannot be sustained. As a result, only a borderline El Niño with maximum warming of the Niño3.4 index in Nov. 2014 occurred (Zhu et al. 2016).

In contrast, in 1997 (Fig. 9), both the zonal atmospheric temperature gradient in the lower troposphere cross the tropical Pacific and vertical temperature anomaly distribution in the troposphere over the central tropical Pacific favored convection development. The fact is that the strongest El Niño in the instrumental record until 2014 was observed in 1997–1998 with maximum warming of the Niño3.4 index in Dec. 1997. Comparing the vertical gradient of the troposphere temperature anomalies in the two specific events, we note that the vertical gradient in boreal summer and autumn (July, September, before

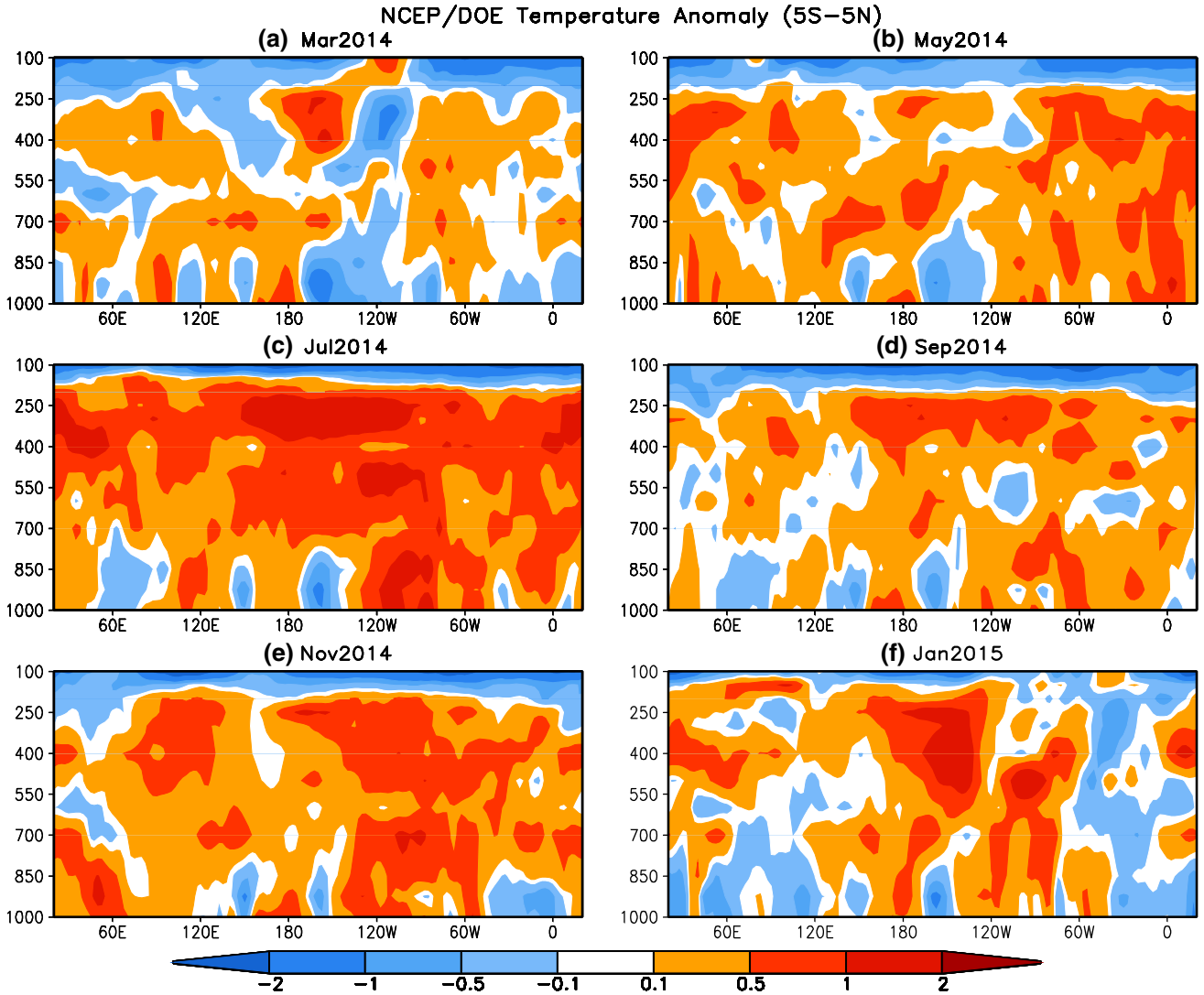

Fig. 8 Air temperature anomaly referred to climatology in 1981–2010 along the equator averaged in 5°S–5°N and in **a** Mar. 2014, **b** May 2014, **c** Jul. 2014, **d** Sep. 2014, **e** Nov. 2014, and **f** Jan. 2015. The unit is °C

climatological peak of an ENSO event or during the development phase of ENSO) displays pronounced contrast (Figs. 8, 9). That is also consistent with the lead-lag correlations shown in Figs. 5b, c, 6, and 7.

3.3 Trend of the atmospheric temperature gradient and its impact on convection

The mean state of tropospheric temperature along the equator experienced a remarkable change during 1979–2014. Figure 10 shows the temperature anomaly averaged over two periods referred to climatology in 1979–2014: 1979–1999 and 2000–2014, as well as their differences and the linear trends during 1979–2014, respectively. The mean anomalies averaged in the two periods are almost mirror image with opposite sign. In contrast to the mean anomaly in 1979–1999 (Fig. 10a), the anomaly averaged for 2000–2014 is slightly larger for both positive and negative anomalies (Fig. 10b). The differences between the two periods (Fig. 10c) are consistent with the linear trends during 1979–2014. The overall troposphere air temperature change pattern is featured by negative (or cold) anomalies mainly around tropopause and positive (or warm) anomalies in the troposphere. The overall anomaly and trend patterns are similar if different reanalysis data are used (not shown), although there are some differences in details.

However, unlike the homogenous cooling trends in the upper troposphere (above 200 hPa), the temperature trends in the middle and lower troposphere show significant regional features (Fig. 10c, d). For example, warm anomalies between 550 and 250 hPa present only over the regions from the Atlantic Ocean to the central and western Pacific.

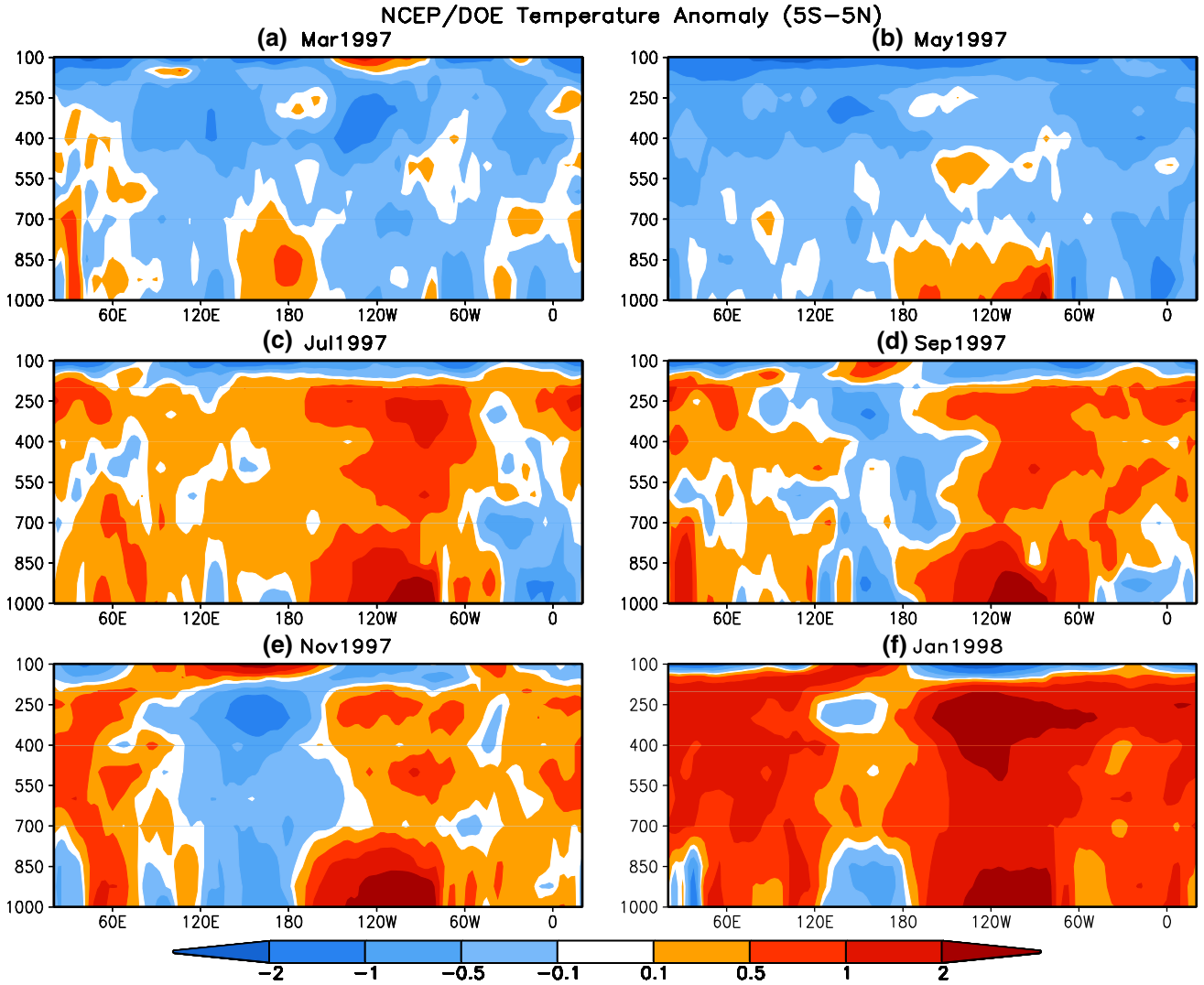

Fig. 9 Air temperature anomaly referred to climatology in 1981–2010 along the equator averaged in 5°S–5°N and in **a** Mar. 1997, **b** May 1997, **c** Jul. 1997, **d** Sep. 1997, **e** Nov. 1997, and **f** Jan. 1998. The unit is °C

The trend is small over the central and eastern Pacific. In the lower troposphere, major warm anomalies occur over the Atlantic and the western Indian Oceans, and centers with weaker warm anomalies exist over the central and western Pacific Ocean. The most interesting feature in the lower troposphere is the pronounced cold anomaly trend over the central and eastern Pacific Ocean. This kind of the distribution of temperature trend forms temperature zonal gradient in the lower troposphere over the Pacific Ocean, which is consistent with strengthening of the Walker circulation as documented by analyzing multi-reanalysis data (Hu et al. 2013b).

The temperature trend pattern shown in Fig. 10 is similar to the spatial pattern of the correlations preceding CP-OLR development shown in Fig. 3a–d, particularly for the Pacific Ocean region. This similarity implies that the long-term trends of the troposphere air temperature for both zonal and vertical gradients along the equator are not favorable for the convection development over the central Pacific. Meanwhile, the wind shear of zonal component between 250 and 1000 hPa in the central and eastern Pacific (140°E–120°W) becomes stronger since 2000 (Fig. 11). That is consistent with the interdecadal change of the mean state in the tropical Pacific, such as the strengthening of the Walker circulation (Hu et al. 2013b). Such wind shear change is also unfavorable for the deep convection development. Thus, long-term trend of the tropospheric atmosphere (e.g., temperature profile and wind shear) change may be one of the possible factors associated with the suppression of convection variability in the central and eastern Pacific (Fig. 12). Without the favorable atmosphere environment for convection development, the atmosphere–ocean coupling or the

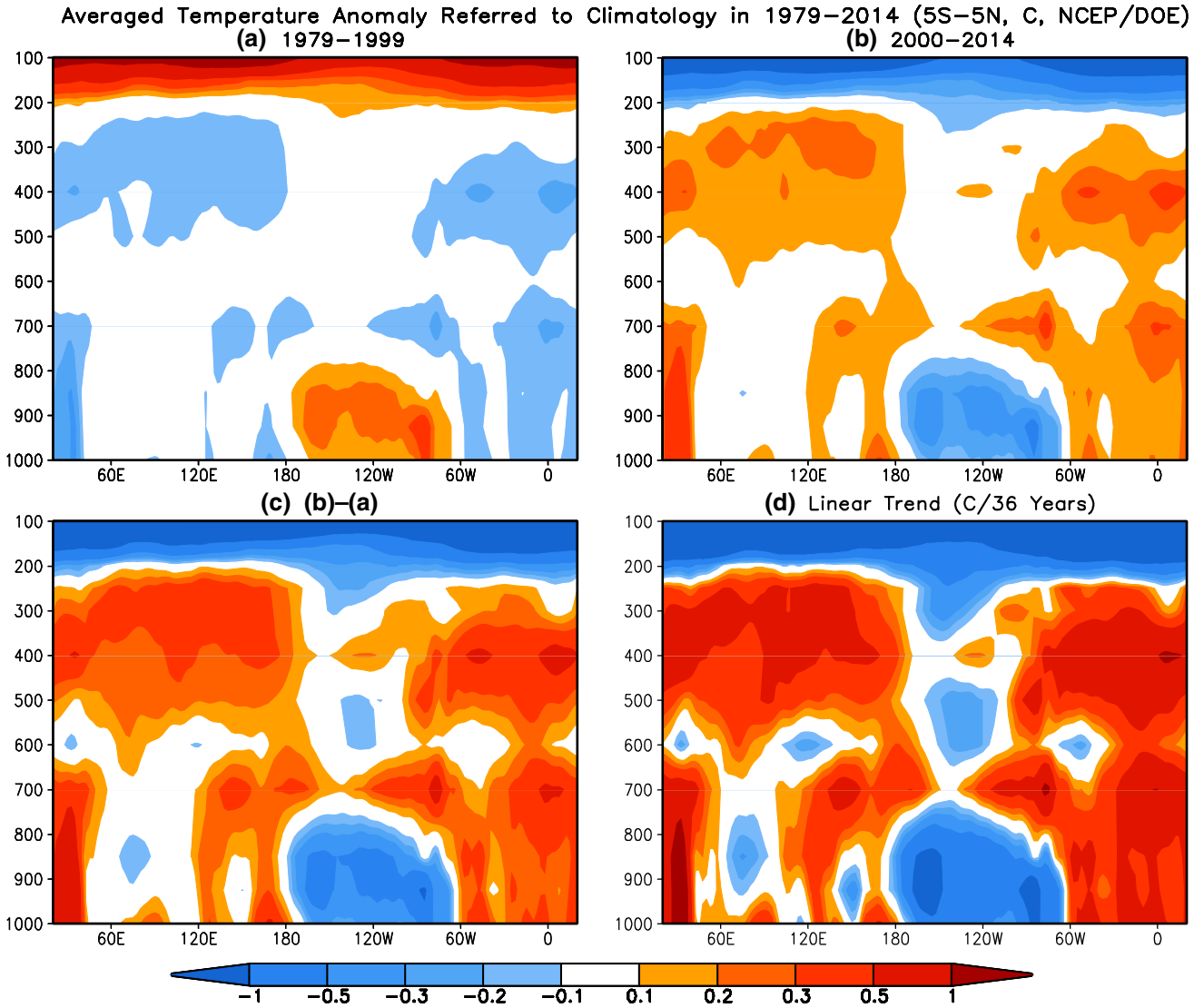

Fig. 10 Air temperature anomaly referred to climatology in 1979–2014 along the equator averaged in 5°S–5°N and in **a** Jan. 1979–Dec. 1999 and **b** Jan. 2000–Dec. 2014, and **c** the differences of **a**, **b**. **d** is the linear trend during Jan. 1979–Dec. 2014. The units are °C in **a**–**c** and °C/36 years in **d**

Bjerknes feedback cannot be sustained. As a result, development of strong El Niño may not be favored, which is consistent with the observational fact that fewer strong El Niño events occurred in 2000–2014.

In fact, this trend pattern (Fig. 10) bears some resemblance to the temperature change caused by the increase of greenhouse gas (GHG) concentrations (Fig. 12 of Chapter 12, IPCC 2013), which may imply some contributions of the increase of GHG concentrations to the observed troposphere air temperature change. Nevertheless, the difference in the tropospheric stability between pre- and post-2000 may also be associated with a phase shift of the interdecadal Pacific Oscillation (IPO), or the so-called hiatus event. Around 1999/2000, IPO shifted from positive phase to negative phase (see Fig. 4 in Henley et al. 2015). It is a further research topic to examine the connection of IPO with mean state change of the tropospheric temperature profile along the equator as well as the interdecadal change of ENSO.

4 Summary and discussion

In this work, we examined the possible connection of troposphere air temperature variation and ENSO evolution as well as the possible impact of long-term trend in tropospheric temperature on ENSO. The lead and lag correlation analyses suggested that in addition to zonal temperature

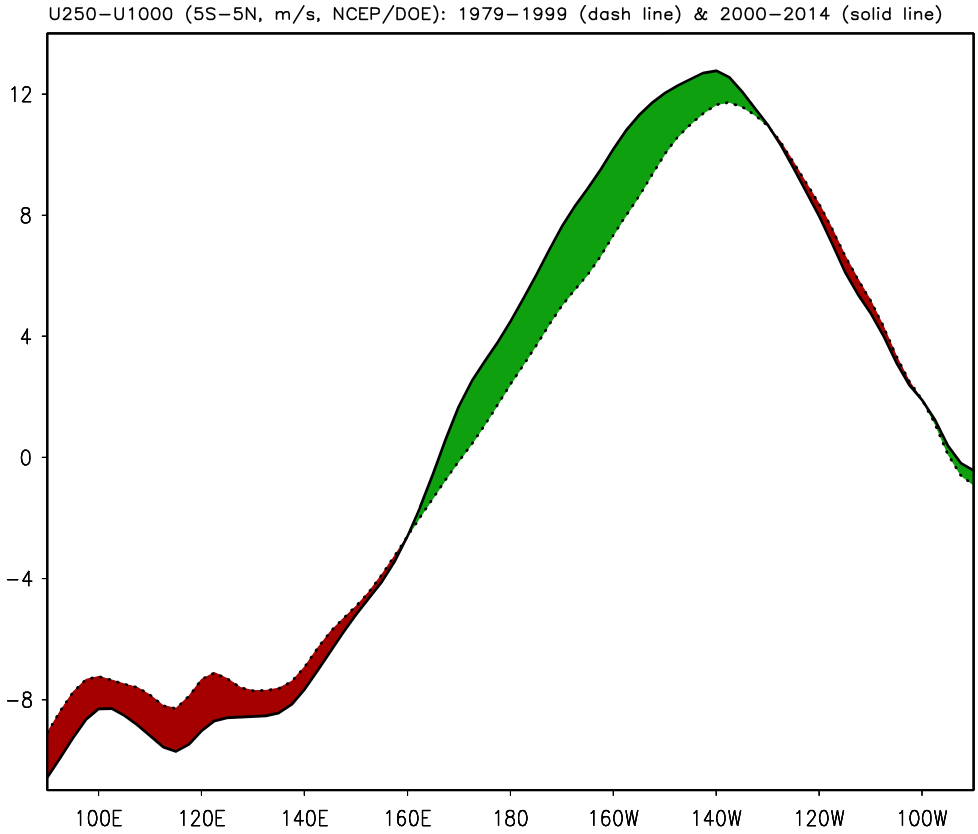

Fig. 11 Wind shear of zonal component between 250 and 1000 hPa (U250-U1000) averaged in 5°S–5°N in Jan. 1979–Dec. 1999 (*dash line*) and Jan. 2000–Dec. 2014 (*solid line*). The unit is m/s. *Green* (*red*) *shading* represents that the wind shear in Jan. 2000–Dec. 2014 is more westerly (easterly) than that in Jan. 1979–Dec. 1999

gradient in lower atmosphere, the troposphere vertical temperature gradient may affect ENSO evolution through enhancement or suppression of convection over the central Pacific. When lower troposphere is relatively warmer (cooler) than upper troposphere, the atmosphere is more (less) unstable and favors the development of an El Niño (a La Niña) event, via enhancement (suppression) of deep convection. This relationship is also consistent with the overall suppression of the variability of tropical Pacific atmosphere and ocean coupled system (including suppressed convections, and reduced ENSO and SST variabilities) in 2000–2014.

Differences in the ENSO evolutions in 1997–1998 and 2014–2015 are found consistent with the statistical relationship. During the springs of 1997 and 2014, there were comparable ocean subsurface warm anomalies along the equator. The contrast of the troposphere atmosphere anomalies seems to be one of the factors leading to different outcomes: the strongest El Niño in the instrumental record in 1997–1998 with profound impact on extra-tropics, and a borderline El Niño in 2014–2025 with little impact on extra-tropics (http://www.climate.gov/news-features/blogs/enso/do-recent-global-precipitation-anomalies-resemble-those-el-ni%C3%B1o). Thus, in addition to the significant and dominant response to ENSO which is largely vertically homogenous in the troposphere, vertical gradient (heterogeneity) of troposphere temperature may play an important and active role to some extent in affecting ENSO evolutions.

It should be pointed out that due to the fact that amplitude of ENSO is controlled by multiple physical processes, the vertical gradient of air temperature in the troposphere is just one possible factor among them. Particularly, since the dominated impact of ENSO on the troposphere temperature, it is a challenge to distinguish the role of the troposphere temperature in affecting convection, from the ENSO-induced other air–sea coupling processes. Our very preliminary work suggested a potentially active role of the atmosphere in ENSO. The vertical temperature gradient in the troposphere may also serve as an intermediate process to enhance or suppress the ENSO development. Clearly, further data analysis, carefully designed model experiments as well as theoretical study are necessary. In addition, it will be a future research topic about the relative importance of lower and upper troposphere temperature variation in the vertical gradient variation as well as the seasonality.

For the long-term trend, the warming is more pronounced in upper troposphere than in the lower troposphere, meaning a reduction of the vertical gradient. Unlike almost homogenous cooling in the upper troposphere, lower troposphere air temperature change along the equator during 1979–2014 shows remarkable regional features.

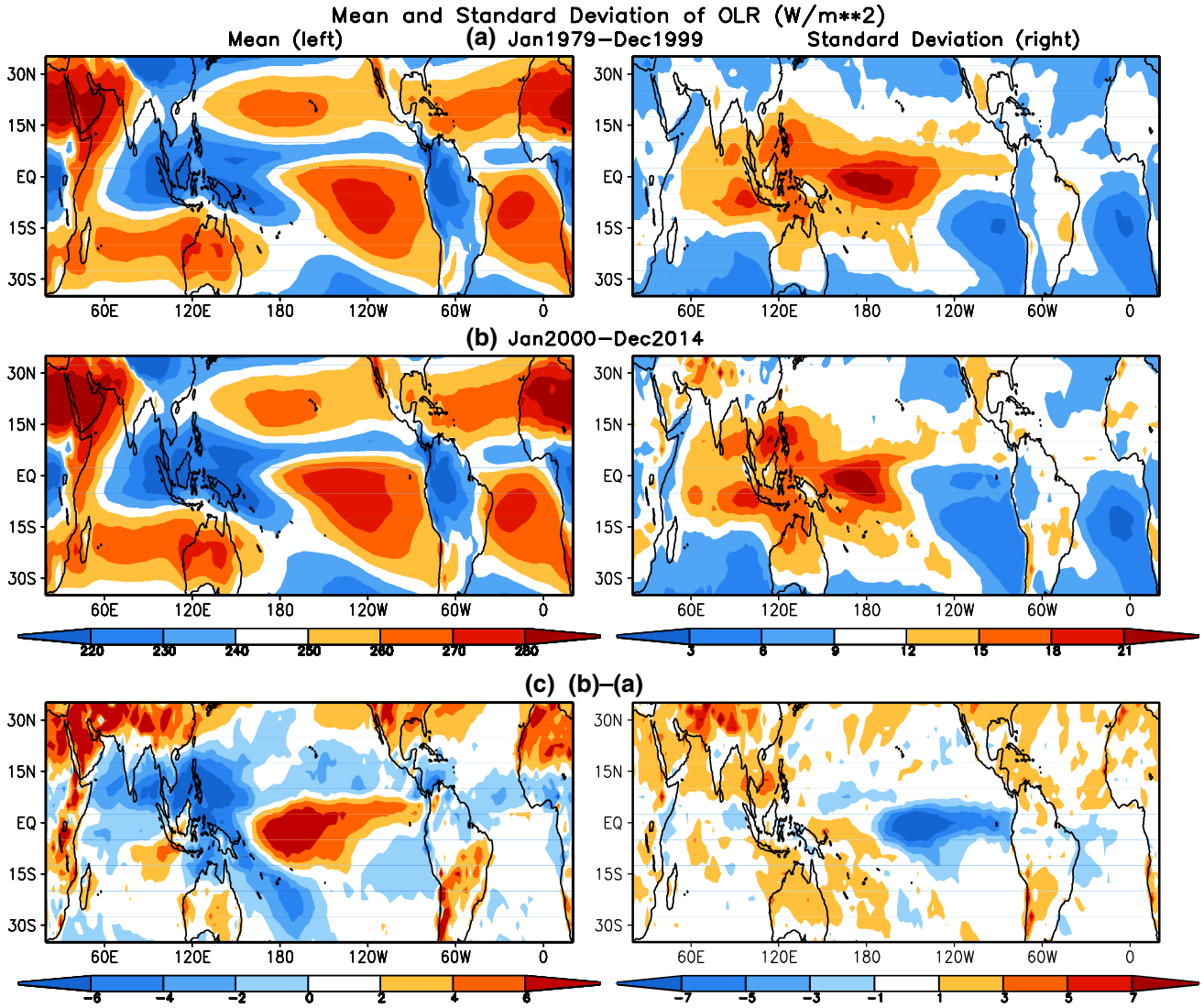

Fig. 12 Mean (*left panels*) and standard deviation (*right panels*) of monthly OLR in **a** Jan. 1979–Dec. 1999 and **b** Jan. 2000–Dec. 2014, and **c** the differences of **a**, **b**. The unit is W/m^2

Strong cooling trend presents over the central and eastern Pacific Ocean, and some warming trend to their two sides, which bears certain resemblance to a La Niña pattern. The lower troposphere warms much less (in fact cools) in the eastern Pacific compared to other regions that suggests the stability there is increasing. According to the lead and lag correlations, this kind of the zonal and vertical distribution of troposphere air temperature trend over the Pacific Ocean is not favorable for convection developments over the central Pacific. Meanwhile, the wind shear in the central and eastern Pacific becomes stronger since 2000 that is also not favorable for the deep convection development. As a consequence of unfavorable atmosphere environment for convection developments, the atmosphere-ocean coupling weakens and strong El Niño is less likely to be generated. However, to make clear, the expected unfavorable long-term trend of tropospheric temperature vertical distribution in global warming scenario does not mean to prevent the happening of strong El Niño; instead, the long-term statistical probability may decrease, since ENSO is determined by complicated physical processes in the ocean and atmosphere other than the sole factor of tropospheric temperature vertical distribution.

Our results suggest that, in addition to the important role played by long-term trend of the atmospheric boundary and ocean, the long-term trend of the tropospheric atmosphere may also play an important and active role to some extent in the ENSO variability suppression in 2000–2014. The role of heterogeneous distribution of atmosphere temperature trend in the lower troposphere on the ENSO

variability change discussed here is consistent with Xiang et al. (2013). They argued that strong divergence in the central Pacific atmospheric boundary layer after the late 1990s prevented the eastward propagation of SST anomalies and results in a more frequent occurrence of central Pacific El Niño and less and weaker eastern Pacific El Niño in the recent decades.

The relationship between the mean state and ENSO feature is a long-time controversial question (Fedorov and Philander 2000; Wang and An 2002; McPhaden et al. 2011; An and Choi 2015). For example, the change in the characteristics of ENSO in 2000–2014, with a preference for La Niña events and fewer large El Niños, may contribute to the increase of contrast between the western and eastern Pacific, such as the east-west gradient in SST and the thermocline (McPhaden et al. 2011; Kumar and Hu 2014; Hu et al. 2013b). Furthermore, it is unclear whether the observed ENSO variability change is just a manifestation of natural variability in the climate system, such as IPO, or it is linked to external forcings. For example, the interdecadal change of ENSO around 1999/2000 is coincident with a shift of IPO from positive phase to negative phase. In addition, in the earlier period (1979–1999), there were two large ENSO events (1982–1983 and 1997–1998), while there was no large ENSO event during 2000–2014. That may be a factor resulting in the linear trends and interdecadal changes of the vertical temperature in the troposphere as well as the heterogeneous distribution of horizontal SST trends. Besides the natural variations, the increase of the GHG concentrations is also a potential contributor to the changes in the mean state and characteristics of ENSO variability (Hu et al. 2012b; Collins et al. 2011; Yeh et al. 2011; Latif and Keenlyside 2008; Meehl et al. 2006; Vecchi et al. 2006; Jin et al. 2001). For instance, under the influence of increase of GHG concentrations, Hu et al. (2012b) showed a weakening of variability associated with ENSO in a coupled model simulation, a scenario consistent with the observed evidence analyzed in this work. Thus, both the natural variability and GHG forced mean state changes may contribute to the observed ENSO variability suppression.

Last, similar to the asymmetric response of convection in the tropical central and eastern Pacific to SST anomaly in warm and cold phases of ENSO as discussed in Hoerling et al. (1997), the connection of vertical temperature gradient with ENSO evolution may also be asymmetric for El Niño and La Niña. It is speculated that the impact of the vertical temperature gradient is more notable in an El Niño development than in a La Niña development, since there are few deep convective activities in the central and eastern Pacific during both climatological state and La Niña. It is also unclear how this asymmetry is associated with possible change of the relationship between the deep convections and ENSO SST. All these deserve further investigations.

Acknowledgements We appreciate the insight comments and constructive suggestions from Dr. Ji Nie and another two reviewers as well as Dr. Peitao Peng. Bohua Huang is supported by grants from NSF (AGS-1338427), NOAA (NA14OAR4310160), and NASA (NNX14AM19G). The scientific results and conclusions, as well as any view or opinions expressed herein, are those of the author(s) and do not necessarily reflect the views of NWS, NOAA, or the Department of Commerce. All the data used in this work are available at NCEP/CPC.

References

An S-I, Choi J (2015) Why the twenty-first century tropical Pacific trend pattern cannot significantly influence ENSO amplitude? Clim Dyn 44(1–2):133–146

Barnston AG, Chelliah M, Goldenberg SB (1997) Documentation of a highly ENSO-related SST region in the equatorial Pacific. Atmos Ocean 35:367–383

Barnston AG, Tippett MK, L'Heureux ML, Li S, DeWitt DG (2012) Skill of real-time seasonal ENSO model predictions during 2002-2011—Is our capability increasing? Bull Am Meteor Soc 93(5):631–651

Bjerknes J (1969) Atmospheric teleconnections from the equatorial Pacific. Mon Wea Rev 97:163–172

Bretherton CS, Widmann M, Dymnikov VP, Wallace JM, Blade I (1999) Effective number of degrees of freedom of a spatial field. J Clim 12:1990–2009

Chiang JCH, Sobel AH (2002) Tropical tropospheric temperature variations caused by ENSO and their influence on the remote tropical climate. J Clim 15:2616–2631

Collimore C, Martin D, Hitchman M, Huesmann A, Waliser D (2003) On the relationship between the QBO and tropical deep convection. J Clim 16(15):2552–2568

Collins M et al (2011) The impact of global warming on the tropical Pacific Ocean and El Niño. Nat Geosci 3:391–397. doi:10.1038/ngeo868

Ding R, Li J, Tseng Y, Sun C, Guo Y (2015a) The Victoria mode in the North Pacific linking extratropical sea level pressure variations to ENSO. J Geophys Res Atmos 120(1):27–45

Ding R, Li J, Tseng Y, Ruan C (2015b) Influence of the North Pacific Victoria mode on the Pacific ITCZ summer precipitation. J Geophys Res Atmos 120(3):964–979

Fedorov AV, Philander SG (2000) Is El Niño changing? Science 288:1997–2002

Guan Y, Zhu J, Huang B, Hu Z-Z, Kinter JL (2014) Southern subtropical Pacific dipole: a predictable mode on multi-seasonal time scales. J Clim 27(4):1648–1658. doi:10.1175/JCLI-D-13-00293.1

Henley BJ, Gergis J, Karoly DJ, Power S, Kennedy J, Folland CK (2015) A tripole index for the interdecadal Pacific oscillation. Clim Dyn 45(11):3077–3090. doi:10.1007/s00382-015-2525-1

Hoerling M, Kumar A, Zhong M (1997) El Niño, La Niña, and the nonlinearity of their teleconnections. J Clim 10:1769–1786

Horii T, Ueki I, Hanawa K (2012) Breakdown of ENSO predictors in the 2000s: decadal changes of recharge/discharge-SST phase relation and atmospheric intraseasonal forcing. Geophys Res Lett 39:L10707. doi:10.1029/2012GL051740

Hu Z-Z, Kumar A, Jha B, Wang W, Huang Bohua, Huang Boyin (2012a) An analysis of warm pool and cold tongue El Niños: air–sea coupling processes, global influences, and recent trends. Clim Dyn 38(9–10):2017–2035. doi:10.1007/s00382-011-1224-9

Hu Z-Z, Kumar A, Jha B, Huang B (2012b) An analysis of forced and internal variability in a warmer climate in CCSM3. J Clim 25(7):2356–2373

Hu Z-Z, Huang B, Kinter JL III, Wu Z, Kumar A (2012c) Connection of stratospheric QBO with global atmospheric general circulation and tropical SST. Part II: interdecadal variations. Clim Dyn 38(1–2):25–43. doi:10.1007/s00382-011-1073-6

Hu Z-Z, Kumar A, Huang B, Wang W, Zhu J, Wen C (2013a) Prediction skill of monthly SST in the North Atlantic Ocean in NCEP Climate Forecast System version 2. Clim Dyn 40(11–12):2745–2756. doi:10.1007/s00382-012-1431-z

Hu Z-Z, Kumar A, Ren H-L, Wang H, L'Heureux M, Jin F-F (2013b) Weakened interannual variability in the tropical Pacific Ocean since 2000. J Clim 26(8):2601–2613. doi:10.1175/JCLI-D-12-00265.1

Hu Z-Z, Kumar A, Huang B, Zhu J, Guan Y (2014) Prediction skill of North Pacific variability in NCEP Climate Forecast System version 2: impact of ENSO and beyond. J Clim 27(11):4263–4272. doi:10.1175/JCLI-D-13-00633.1

Hu Z-Z, Kumar A, Huang B (2016) Spatial distribution and the interdecadal change of leading modes of heat budget of the mixed-layer in the tropical Pacific and the association with ENSO. Clim Dyn 46(5–6):1753–1768. doi:10.1007/s00382-015-2672-4

Huang B, Hu Z-Z, Kinter JL III, Wu Z, Kumar A (2012) Connection of stratospheric QBO with global atmospheric general circulation and tropical SST. Part I: methodology and composite life cycle. Clim Dyn 38(1–2):1–23. doi:10.1007/s00382-011-1250-7

IPCC (2013) Climate Change 2013: The Physical Science Basis. In: Stocker TF et al. (eds) Contribution of Working Group I to the Fifth Assessment Report of the Intergovernmental Panel on Climate Change. Cambridge University Press, Cambridge, United Kingdom and New York, NY, USA, 1535 pp

Jiang X, Yang S, Li J, Li Y, Hu H, Lian Y (2013) Variability of the Indian Ocean SST and its possible impact on summer western North Pacific anticyclone in the NCEP Climate Forecast System. Clim Dyn 41(7–8):2199–2212

Jin F-F, Hu Z-Z, Latif M, Bengtsson L, Roeckner E (2001) Dynamics and cloud-radiation feedbacks in El Niño and greenhouse warming. Geophys Res Lett 28(8):1539–1542

Kanamitsu M, Ebisuzaki W, Woollen J, Yang S-K, Hnilo JJ, Fiorino M, Potter GL (2002) NCEP-DOE AMIP-II Reanalysis (R-2). Bull Am Meteor Soc 83:1631–1643

Kumar A, Hoerling MP (2003) The nature and causes for the delayed atmospheric response to El Nino. J Clim 16:1391–1403

Kumar A, Hu Z-Z (2014) Interannual and interdecadal variability of ocean temperature along the equatorial Pacific in conjunction with ENSO. Clim Dyn 42(5–6):1243–1258. doi:10.1007/s00382-013-1721-0

Kumar A, Wang H, Xue Y, Wang W (2014a) How much of monthly subsurface temperature variability in the equatorial Pacific can be recovered by the specification of sea surface temperatures? J Clim 27:1559–1577. doi:10.1175/JCLI-D-13-00258.1

Kumar A, Jha B, Wang H (2014b) Attribution of SST variability in global oceans and the role of ENSO. Clim Dyn 43:209–220. doi:10.1007/s00382-013-1865-y

Kumar A, Chen M, Xue Y, Behringer D (2015) An analysis of the temporal evaluation of ENSO prediction skill in the context of equatorial Pacific ocean observing system. Mon Wea Rev 143:3204–3213

L'Heureux ML, Tippett MK, Barnston AG (2015) Characterizing ENSO coupled variability and its impact on North American seasonal precipitation and temperature. J Clim 28:4231–4245. doi:10.1175/JCLI-D-14-00508.1

Latif M, Keenlyside N (2008) El Niño/Southern Oscillation response to global warming. Proc Natl Acad Sci 106(49):20578–20583. doi:10.1073/pnas.0710860105

Liebmann B, Smith CA (1996) Description of a complete (interpolated) outgoing long wave radiation dataset. Bull Am Meteor Soc 77:1275–1277

McPhaden MJ (2012) A 21st century shift in the relationship between ENSO SST and warm water volume anomalies. Geophys Res Lett 39:L09706. doi:10.1029/2012GL051826

McPhaden MJ, Lee T, McClurg D (2011) El Niño and its relationship to changing background conditions in the tropical Pacific Ocean. Geophys Res Lett 38:L15709. doi:10.1029/2011GL048275

Meehl GA, Teng H, Branstator G (2006) Future changes of El Niño in two global coupled climate models. Clim Dyn 26(6):549. doi:10.1007/s00382-005-0098-0

National Research Council (2010) Assessment of intraseasonal to interannual climate prediction and predictability, 192 pp, ISBN-10: 0-309-15183-X, the National Academies Press, Washington, DC, USA

Nie J, Sobel AH (2015) Responses of tropical deep convection to the QBO: cloud-resolving simulations. J Atmos Sci 72(9):3625–3638

Pedhazur EJ (1997) Multiple regression in behavioural research: explanation and prediction, 3rd edn. Holt Rinchart & Winston, Austin

Rasmusson EM, Carpenter TH (1982) Variation in tropical sea surface temperature and surface wind fields associated with Southern Oscillation/El Niño. Mon Wea Rev 110:354–384

Reynolds RW, Rayner NA, Smith TM, Stokes DC, Wang W (2002) An improved in situ and satellite SST analysis for climate. J Clim 15:1609–1625

Saha S et al (2006) The NCEP climate forecast system. J Clim 19:3483–3517

Sobel AH, Held IM, Bretherton CS (2002) The ENSO signal in tropical tropospheric temperature. J Clim 15:2702–2706

Vecchi GA et al (2006) Weakening of tropical Pacific atmospheric circulation due to anthropogenic forcing. Nature 441:73–76

Wang B, An S-I (2002) A mechanism for decadal changes of ENSO behavior: roles of background wind changes. Clim Dyn 18:475–486

Wang W, Chen M, Kumar A (2010) An assessment of the CFS real-time seasonal forecasts. Wea Forecast 25:950–969. doi:10.1175/2010WAF2222345.1

Xiang B, Wang B, Li T (2013) A new paradigm for the predominance of standing Central Pacific warming after the late 1990s. Clim Dyn 41(2):327–340. doi:10.1007/s00382-012-1427-8

Yeh S-W, Kirtman BP, Kug J-S, Park W, Latif M (2011) Natural variability of the central Pacific El Niño event on multi-centennial timescales. Geophys Res Lett 38:L02704. doi:10.1029/2010GL045886

Zhu J, Kumar A, Huang B, Balmaseda MA, Hu Z-Z, Marx L, Kinter JL III (2016) The role of off-equatorial surface temperature anomalies in the 2014 El Niño prediction. Sci. Rep. 6:19677. doi:10.1038/srep19677